

RESEARCH LETTER

10.1002/2017GL075958

Key Points:

- We present the first quantitative assessment of the algal contribution to the Greenland ice sheet surface darkening
- We found that the effect of algae on bare ice darkening in the study area is greater than that of nonalgal impurities
- Incorporating the darkening effect of ice algal growth will improve mass balance and sea level projections of the Greenland ice sheet

Supporting Information:

- Supporting Information S1
- Data Set S1

Correspondence to:

M. Stibal and J. E. Box,
marek.stibal@natur.cuni.cz;
jeb@geus.dk

Citation:

Stibal, M., Box, J. E., Cameron, K. A., Langen, P. L., Yallop, M. L., Mottram, R. H., ... Ahlström, A. P. (2017). Algae drive enhanced darkening of bare ice on the Greenland ice sheet. *Geophysical Research Letters*, 44. <https://doi.org/10.1002/2017GL075958>

Received 6 OCT 2017






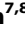











Accepted 1 NOV 2017

Accepted article online 6 NOV 2017

©2017. The Authors.

This is an open access article under the terms of the Creative Commons Attribution-NonCommercial-NoDerivs License, which permits use and distribution in any medium, provided the original work is properly cited, the use is non-commercial and no modifications or adaptations are made.

Algae Drive Enhanced Darkening of Bare Ice on the Greenland Ice Sheet

Marek Stibal^{1,2} , Jason E. Box³ , Karen A. Cameron^{1,4} , Peter L. Langen⁵ , Marian L. Yallop⁶ , Ruth H. Mottram⁵ , Alia L. Khan^{7,8,9} , Noah P. Molotch^{8,10} , Nathan A. M. Christmas¹¹ , Filippo Cali Quaglia^{3,12} , Daniel Remias¹³ , C. J. P. Paul Smeets¹⁴ , Michiel R. van den Broeke¹⁴ , Jonathan C. Ryan¹⁵ , Alun Hubbard¹⁵ , Martyn Tranter¹¹ , Dirk van As³, and Andreas P. Ahlström³ 

¹Department of Geochemistry, Geological Survey of Denmark and Greenland, Copenhagen, Denmark, ²Department of Ecology, Faculty of Science, Charles University, Prague, Czechia, ³Department of Glaciology and Climate, Geological Survey of Denmark and Greenland, Copenhagen, Denmark, ⁴Institute of Biological, Environmental and Rural Sciences, Aberystwyth University, Aberystwyth, UK, ⁵Danish Meteorological Institute, Copenhagen, Denmark, ⁶School of Biological Sciences, University of Bristol, Bristol, UK, ⁷Department of Civil and Environmental Engineering, Institute of Arctic and Alpine Research, University of Colorado Boulder, Boulder, CO, USA, ⁸Department of Geography, Institute of Arctic and Alpine Research, University of Colorado Boulder, Boulder, CO, USA, ⁹Now at The National Snow and Ice Data Center and Cooperative Institute for Research in Environmental Sciences at the University of Colorado Boulder, Boulder, CO, USA, ¹⁰Jet Propulsion Laboratory, California Institute of Technology, Pasadena, CA, USA, ¹¹School of Geographical Sciences, University of Bristol, Bristol, UK, ¹²Department of Physics, University of Turin, Turin, Italy, ¹³School of Engineering and Applied Natural Sciences, University of Applied Sciences Upper Austria, Wels, Austria, ¹⁴Institute for Marine and Atmospheric Research, Utrecht University, Utrecht, Netherlands, ¹⁵Institute of Geography and Earth Sciences, Aberystwyth University, Aberystwyth, UK

Abstract Surface ablation of the Greenland ice sheet is amplified by surface darkening caused by light-absorbing impurities such as mineral dust, black carbon, and pigmented microbial cells. We present the first quantitative assessment of the microbial contribution to the ice sheet surface darkening, based on field measurements of surface reflectance and concentrations of light-absorbing impurities, including pigmented algae, during the 2014 melt season in the southwestern part of the ice sheet. The impact of algae on bare ice darkening in the study area was greater than that of nonalgal impurities and yielded a net albedo reduction of 0.038 ± 0.0035 for each algal population doubling. We argue that algal growth is a crucial control of bare ice darkening, and incorporating the algal darkening effect will improve mass balance and sea level projections of the Greenland ice sheet and ice masses elsewhere.

Plain Language Summary Melting of the Greenland ice sheet is enhanced by surface darkening caused by various impurities. We quantified the contribution of dark pigment-producing algae to the ice sheet surface darkening, based on field measurements in the southwestern part of the ice sheet during the 2014 melt season. Our analysis reveals that the impact of algae on bare (snow-free) ice darkening was greater than that of other impurities and, therefore, that algal growth was a crucial control of bare ice darkening in the study area. Incorporating the darkening effect of algal growth is expected to improve future projections of the Greenland ice sheet melting.

1. Introduction

Surface melting of the Greenland ice sheet is enhanced by darkening due to liquid water, snow grain metamorphism, and light-absorbing impurities (LAI) (Fettweis et al., 2011; Tedesco et al., 2016). LAI include mineral dust (Bøggild et al., 2010; Doherty et al., 2010; Wientjes et al., 2011), black carbon (Doherty et al., 2013, 2010; Keegan et al., 2014), and pigmented microbial cells (Yallop et al., 2012). Microbes that colonize glacier surfaces have the potential to increase in biomass and thus darkening impact given liquid water, sunlight, and nutrients (Stibal et al., 2012). By contrast, the potential of other LAI to increase their darkening impact once accumulated on the ice surface is limited.

Algae from the group Zygnematophyceae ("surface ice algae") are abundant on the surface of the ice sheet (Yallop et al., 2012). Surface ice algae produce dark pigments as a screening mechanism when exposed to the high-intensity radiation typical of glacier environments (Remias, Holzinger, et al., 2012; Remias, Schwaiger, et al., 2012). Humic by-products of microbial metabolism absorb in the same optical wavelengths and may

further contribute to the darkening (Takeuchi, 2002; Takeuchi et al., 2015). The impact of microbes on ice surface albedo is the least understood and quantified melt-enhancing factor on the ice sheet (Benning et al., 2014; Stibal et al., 2012).

Every summer, a dark area appears along the western margin of the ice sheet between 65 and 70°N (Shimada et al., 2016; Wientjes & Oerlemans, 2010). Previously, the low bare ice albedo has been attributed to outcropping dust and black carbon (Goelles et al., 2015; Wientjes et al., 2011). However, high abundances of surface ice algae have also been observed in this area (Yallop et al., 2012). To quantify the algal contribution to the ice surface darkening, we chose a study site at the edge of this dark area and, over ~2 months in the summer 2014, we determined the changing surface albedo, measured the abundance of surface ice algae and other LAI, and obtained simultaneous reflectance spectra in the study site. We also gathered surface ice samples from outside the dark area to demonstrate the ubiquitous presence of surface ice algae and assess the environmental factors controlling their abundance. We then quantified the relationship between algae and non-algal LAI and bare ice darkening.

2. Materials and Methods

2.1. Field Site

The study site was located in the southwestern sector of the Greenland ice sheet near the automated climate station S6 at 67° 04.779'N, 49° 24.077'W, and 1,011 m above sea level (van den Broeke et al., 2011; supporting information Figure S1). Field measurements and sampling were conducted over 56 days from 17 June to 11 August 2014 (day of year 168–223). At the start of the survey (17 June), the ice surface was covered in 10–30 cm deep snow, and our first LAI concentration and spectral reflectance measurements were therefore made for melting snow. On 19 June, the first bare ice was exposed and in the first week we performed surface reflectance and albedo measurements and collected samples of snow, surface streams and pools, and clean, medium, and dark ice to quantify the full variability of surface types in the study area. From 1 July to 11 August a 20 × 20 m study site was established, and on each sampling day 10 randomly selected 1 × 1 m sampling plots were targeted to capture average changes in surface reflectance over time while avoiding sample location bias and/or disturbance. Digital images of the study area were acquired by a Sony NEX-5N camera mounted on a fixed-wing unmanned aerial vehicle (UAV) (Ryan et al., 2015). Each image was georeferenced with the GPS and attitude data. A total of 780 overlapping images at an altitude of 300 m above the ice surface was obtained.

Additional samples to determine algal abundance and biovolume in surface ice were collected at other locations on the ice sheet during the summer 2013 (supporting information Figure S2). Most sites were in the vicinity of an automated climate station of the Programme for the Monitoring of the Greenland Ice sheet network (Ahlstrøm et al., 2008; van As et al., 2016). Samples were also taken at the “dark site” (DS), one of the darkest 5 km pixels from optical satellite imagery (Box et al., 2012). Details of the sites can be found in Stibal et al. (2015).

2.2. Surface Reflectance and Albedo Measurements

Spectral reflectance in the range of 350–2,500 nm was acquired using an Analytical Spectral Devices (ASD) Field Spectrometer 2 with a hemispheric cosine receptor. The instrument was leveled sighting a bubble in a fluid chamber to an accuracy of 1°. The effective footprint of the sensor held at hip height was ~80 cm in diameter, with a 120° cone giving ~80% of the incident energy. The measurements were based on a ratio of upward to downward facing measurements made within 2 h of local solar noon. A variety of surfaces were sampled, spanning 0.4 m deep meltwater stream at the low albedo limit to 1 mm grain ~10 day old snow at the high limit. To estimate broadband albedo, the spectral reflectance values were weighted by downward solar spectrum values calculated using SBDART (Ricchiuzzi et al., 1998) with inputs of observed cloud fraction and climatological values for ozone, water vapor, and aerosol optical depth after Box (1997).

2.3. Sample Collection and Analysis

Samples of surface (2–3 cm) snow and ice were collected from a 0.4 × 0.4 m area using a chisel and pre-cleaned with 10% HCl and 70% ethanol, from the area over which reflectance measurements were acquired. The samples were allowed to thaw at <15°C and between 0.5 and 30 mL of the sample was filtered through a 0.22 μm Whatman Nucleopore polycarbonate membrane filter, depending on sample turbidity. Algal cells

were counted in 5–20 fields of view at a 160X magnification using a Bresser Biolux NV field microscope. Unfiltered sample (40 mL) was fixed with formaldehyde (final concentration 2% vol/vol) and stored at $<5^{\circ}\text{C}$ for further analysis. The rest of each sample was filtered through a preweighed $0.45\ \mu\text{m}$ Whatman cellulose nitrate membrane filter for total suspended solids (TSS) analysis. HCl- and ethanol-sterilized gloves were worn throughout all sample handling.

Separate samples were collected in precleaned and combusted amber glass bottles for black carbon (BC) analysis just prior to scheduled helicopter flights to minimize sample melting prior to processing. The samples were melted upon arrival in the laboratory and immediately aerosolized with a calibrated CETAC U5000 nebulizer. Refractory BC (rBC) concentrations in the samples were determined using a single particle soot photometer (SP2), which measures single-particle incandescence of rBC at 1,064 nm. The SP2 was calibrated with fullerene soot (Lot F12S011; Alfa Aesar) and applied over masses of 1–20 fg (Baumgardner et al., 2012). The resulting linear calibration was extrapolated to large rBC masses using a power law dependence of $1/(0.9)$ (Schwarz et al., 2012).

Formaldehyde-preserved samples were examined by light microscopy for algal species identification, quantification of cell abundance, and determination of cell size and biovolume. A Leica DM LB2 light microscope was used at a magnification of 400X and 1,000X. Biovolume was determined using an appropriate geometric model (Hillebrand et al., 1999). At least 50 cells of each algal species were measured. The concentration of total suspended solids (TSS) was determined by filtering samples through preweighed $0.45\ \mu\text{m}$ cellulose nitrate membrane filters and reweighing them after oven drying at 90°C for 5 h. The nonalgal LAI fraction (NA; $\mu\text{g mL}^{-1}$) of the TSS was estimated as $\text{NA} = \text{TSS} - (\text{B} \times \text{C})$, where B is cell biomass in $\mu\text{g cell}^{-1}$ and C is cell abundance in cells mL^{-1} . Wet biomass of the algae was calculated from their biovolume, assuming neutral buoyancy of the algal cells; dry biomass was estimated as 50% of wet biomass. We tested the sensitivity of the calculated nonalgal fraction concentration, its proportion in TSS, and the calculated correlations with albedo to the cell biomass estimates. This analysis suggested that a biomass between 1 and 5 ng dry weight per cell is a realistic estimate (supporting information Figure S3), which agrees with an estimate of 3 ng wet weight obtained from a laboratory analysis of preserved ice samples.

2.4. Data Analysis

To quantitatively assess the relationship between the algal and nonalgal LAI concentrations and ASD-derived surface reflectance measured at the study site in the summer 2014, a linear regression analysis was performed using all samples for which reflectance, algal abundance, and TSS concentration data were available ($n = 93$). Binary logarithms of algal abundance and nonalgal LAI concentrations were used as the absorption of solar radiation by particles, including algal cells, is directly proportional to their mass absorption cross section. The resulting linear regression assumes the form $\alpha = \alpha_0 + s \times C$, where α is the reflectance (relative units), C the binary logarithm of cell abundance in $10^3\ \text{cells mL}^{-1}$ or the nonalgal fraction concentration in $\mu\text{g mL}^{-1}$, α_0 is the initial no-algae bare ice reflectance, and s is the function multiplier.

We applied redundancy analysis to explain the variation in the ASD-derived reflectance data collected at the study site in the summer 2014 and in the algal abundance and biovolume data from the far-field samples collected around the ice sheet in the summer 2013. For the former, ASD-derived reflectance data averaged over 10 nm increments were the response variables; day of year 2014, days since the last precipitation event, nonalgal fraction concentration, and algal abundance were the explanatory variables. For the latter, algal abundance and biovolume were the response data; geographical position, altitude, distance from the margin of the ice sheet, surface type (firn and ice), positive screen-level air temperature (T_a) days and days of surface temperature (T_s) of 0° since the beginning of the year, days since the last precipitation event, dust, and nitrate concentrations were the explanatory data; day of sampling (day of year 2013) was a covariate. All concentration, microbial abundance, and biovolume data were log-transformed prior to analysis, and all data were standardized and centered. Data below detection limit were treated as zeroes. The p values were corrected for multiple testing using false discovery rate.

To estimate the doubling time for the algal population, a linear regression was performed using samples from the random plots where bare ice reflectance and algal abundance were available. Based on the assumption that algae are buried by snow or washed away by rain, we classified the days after precipitation events as the start-up dates for population growth. The resulting linear regression takes the form of $C = C_0 + \text{GR} \times \text{DSP}$,

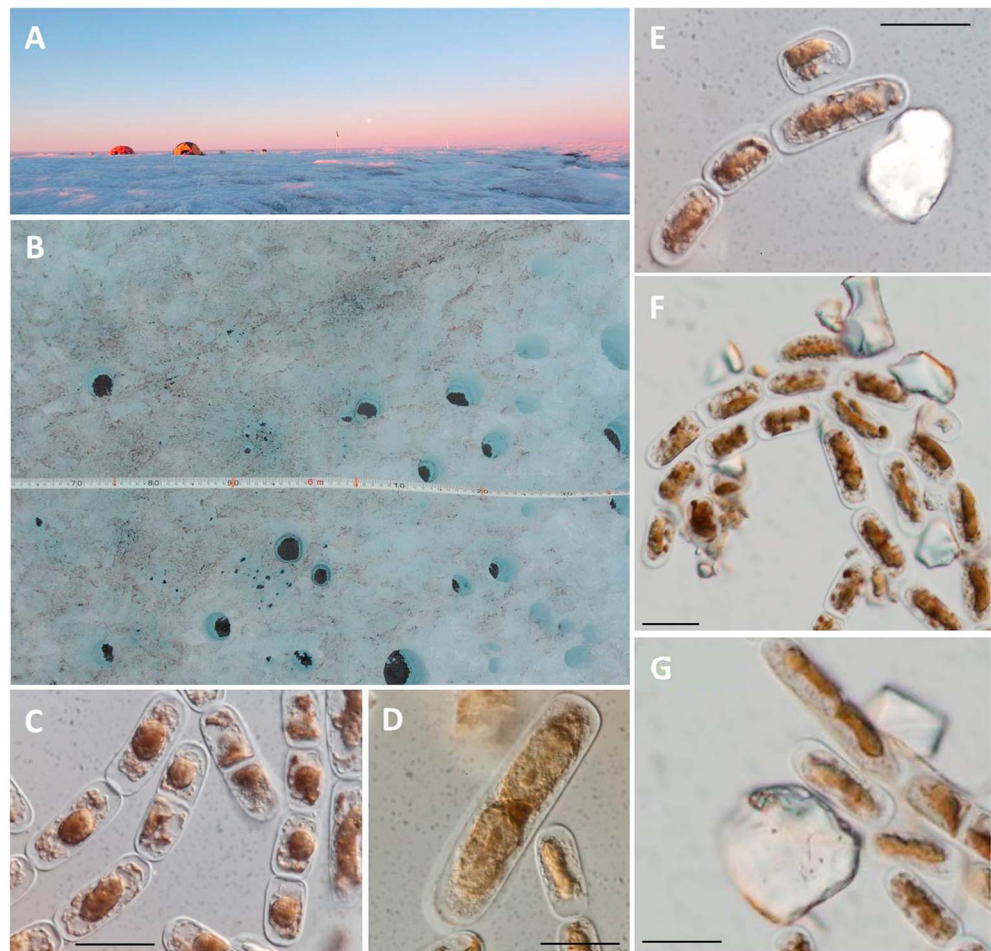


Figure 1. Observing surface ice algae on the Greenland ice sheet. (a) The principal study site. (b) The ice sheet surface showing highly pigmented surface blooms. Photomicrographs of cells of the filamentous alga *Ancydonema nordenskiöldii* in various stages of (c) cell elongation and cell division, (d) terminal cell of a filament of *A. nordenskiöldii* alongside a much larger cell of *Cylindrocystis* sp., and (e–g) translucent mineral particles contrasting in absorbance with pigmented algal cells. Scale bars represent 20 μm . All samples were preserved in 2% formaldehyde resulting in some loss of pigment and shrunken protoplasts.

where C is the binary logarithm of cell abundance in 10^3 cells mL^{-1} , DSP the number of days since a precipitation event as simulated in the ERA-Interim-driven regional climate model HIRHAM5 (Langen et al., 2015), C_0 is the calculated initial cell abundance, and GR is the growth rate calculated from the slope of the linear fit. Algal population doubling time was subsequently determined as $1/\text{GR}$.

3. Results

3.1. Bare Ice Albedo

After winter snowpack had completely ablated, surface albedo (α) decreased from 0.50 to 0.42 ($\Delta\alpha = -0.08 \pm 0.04$) in the 35 days of observation at the S6 climate station (from 7 July to 11 August; day of year 188–223). Over the same time period, NASA Moderate Resolution Imaging Spectroradiometer MOD10A1 daily gridded albedo data indicate a mean albedo decline from 0.42 to 0.38 ($\Delta\alpha = -0.04 \pm 0.05$) at the nearest 500 m MOD10A1 pixel and from 0.43 to 0.37 ($\Delta\alpha = -0.06 \pm 0.05$) in a 10 km radius area of MOD10A1 pixels located 13.5 km northeast of the S6 climate station (supporting information Figure S1). UAV imagery indicates that snow cover was completely absent from the study area in early August and that surface meltwater covered a fractional area of only 4% (supporting information Figure S4).

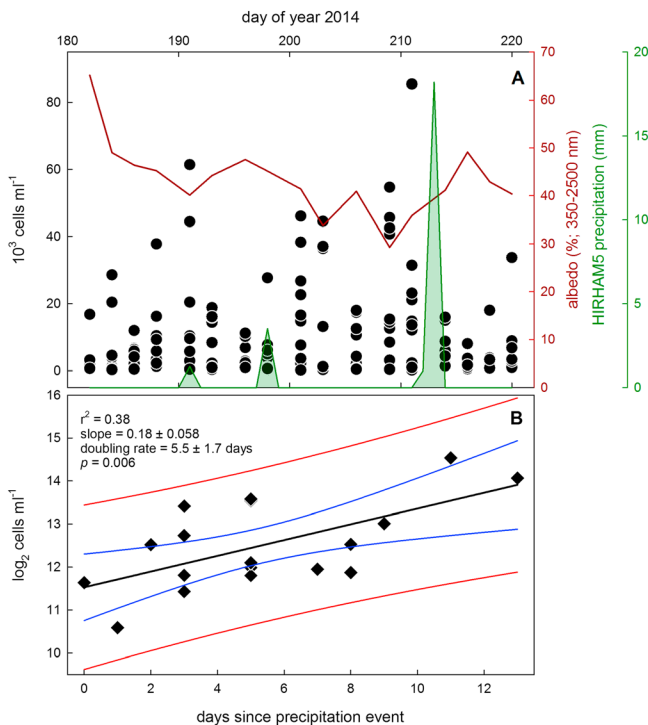


Figure 2. Surface ice algal abundance dynamics on the Greenland ice sheet. (a) Algal abundance at 10 random plots in the study area sampled each day, ASD-derived albedo (350–2,500 nm), and precipitation data from the HIRHAM5 regional climate model. All precipitation was rain during the measurement period. (b) Algal doubling time estimated on the basis of the relationship between the binary logarithm of mean algal abundance and the time elapsed since the last precipitation event. 95% confidence and prediction bands marked in blue and red, respectively.

3.2. Surface Ice Algae

At melt onset, we observed dead algal cells and other dark material being transported with slush and meltwater flow (supporting information Figure S5). After melting and runoff from winter snow and slush had completely ceased from the study site, we detected the first live algal cells in the surface ice (Figure 1). The distribution of surface ice algae in the principal study area was patchy, as demonstrated by the large spatial variation in abundance within the sampling area of 20×20 m (Figure 2). The abundance of algal cells ranged from <100 to $85,000 \text{ mL}^{-1}$ of melted ice in the sampling plots (Figure 2a) and up to $180,000 \text{ cells mL}^{-1}$ at sample sites selected for their dark appearance. Three species of algae were identified in the samples based on their morphology: *Ancylonema nordenskiöldii*, usually the dominant component of the community (40–100% of cells observed), *Mesotaenium berggrenii* reaching up to 50%, and *Cylindrocystis* sp. (Figure 1). By contrast, cyanobacterial filaments were only observed in low numbers. Observations of dividing cells (Figures 1c–1g) confirm active growth of algae in surface ice occurred. Algal growth, as demonstrated by the increase in abundance through time (Figure 2a), appeared to be moderated by rainfall events. This is supported by the significant correlation between the number of days since the last precipitation event and algal abundance in the study area (Figure 2b). Redundancy analysis performed to explain the variation in algal abundance and biovolume data from around the ice sheet (supporting information Table S1) identified the time since the last precipitation event as a significant factor (supporting information Table S2). We attribute this effect to the flushing of algae into cryoconite holes and supraglacial stream channels during rainfall events. Assuming uninterrupted algal growth between the observed precipitation events in our study area, the mean time for doubling of the population size was estimated to be 5.5 ± 1.7 days (Figure 2b).

3.3. Reflectance Spectra

The field spectrometer-obtained optical reflectance spectra (Figure 3a) indicate the surface ice in the principal study area contained a mixture of microbial pigments and humic substances. An absorption feature at ~ 680 nm (Figure 3b) is attributed to algal chlorophyll (Bidigare et al., 1990; Painter et al., 2001), while algal chlorophylls and carotenoids likely cause the absorption features between 370 and 680 nm (Bidigare et al., 1990). The absorption peaking at 576 nm (Figure 3b) could be attributed to phycoerythrin produced by cyanobacteria (Bryant, 1982), common microbes on the Greenland ice sheet surface (Stibal et al., 2010; Wientjes et al., 2011; Yallop et al., 2012). However, cyanobacteria were only detected in low numbers, and the identity of this peak thus remains inconclusive. Distinct peaks of spectral absorption features are likely masked by humic substances (Takeuchi, 2002) and factors such as snow and ice grain size, solar angle, and liquid water (Hadley & Kirchstetter, 2012). The brown-colored protective pigments produced by surface ice algae have their main absorption peaks below 350 nm (Remias, Holzinger, et al., 2012; Remias, Schwaiger, et al., 2012), and these peaks were not detectable with the ASD spectrometer used. BC, which absorbs across the visible spectrum with no discernible spectral absorption peaks (Bond & Bergstrom, 2006), was also detected in our samples at concentrations between 2.9 ng g^{-1} in fresh snow and clean ice and 32 ng g^{-1} in dark ice with high impurity contents (supporting information Table S3). The role of dust in the reflectance spectra was likely small compared with biotic absorbers, as demonstrated by Yallop et al. (2012).

3.4. Light-Absorbing Impurities and Surface Reflectance

We divided the LAI in the surface ice samples into algal and nonalgal fractions to examine their respective roles in the observed surface darkening. Bare ice albedo was then correlated to the binary logarithms of

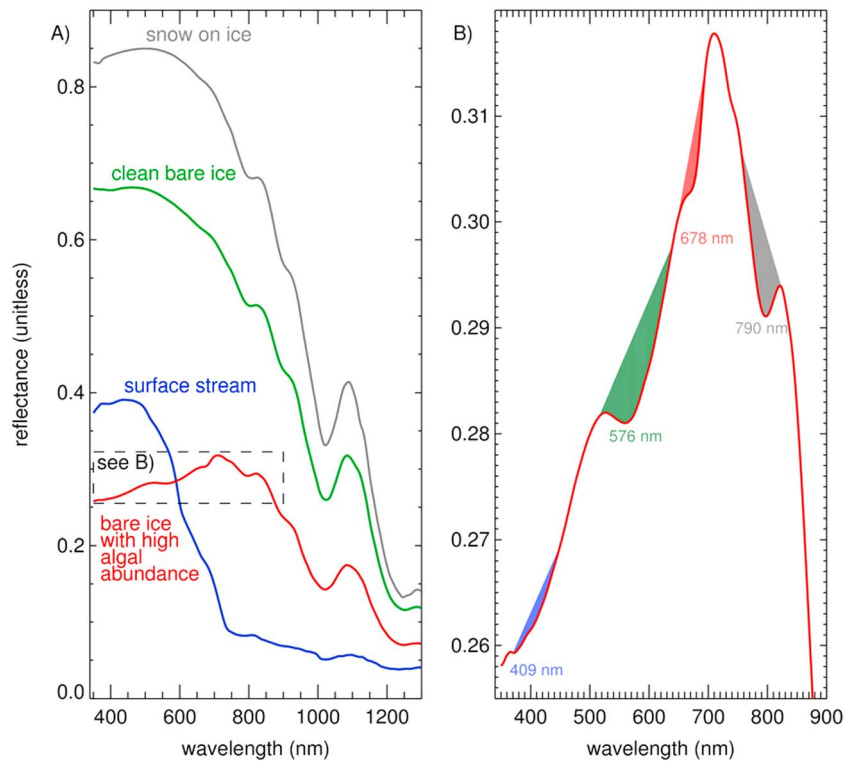


Figure 3. Reflectance spectra of Greenland surface ice. (a) Spectra of representative surfaces. Surface meltwater stream depth was 1 m. Snow depth was 24 cm with ~ 0.6 mm grain diameter, estimated from visual inspection. (b) Spectral reflectance of surface ice with high algal abundance showing four apparent absorption features with peak absorption wavelength computed from continuum reflectance model (Painter et al., 2001). The 409 and 678 nm absorption features match the typical chlorophyll and carotenoid absorption values (Bidigare et al., 1990). The absorption peaking at 576 nm might be attributed to phycoerythrin (Bryant, 1982). The 790 nm absorption feature is likely abiotic. Each curve represents single pairs of ratios of upward and downward measured spectra. A low-pass Gaussian weighted smoothing filter was applied to the shown spectra.

algal abundance and the nonalgal fraction concentration. Using samples from the random plots, we found a significant negative correlation between algal abundance and albedo, which was strongest in the visible wavelengths (Pearson's $r = -0.78$, $p < 0.0001$ for 350–750 nm). The broadband albedo sensitivity (Pearson's $r = -0.75$, $p < 0.0001$ for 350–2,500 nm) was stronger than that of the nonalgal fraction (Pearson's $r = -0.47$, $p < 0.0001$ for 350–750 nm; Pearson's $r = -0.45$, $p < 0.0001$ for 350–2,500 nm; Figure 4; supporting information Table S4). Algal abundance correlated best with surface reflectance between 350 and 600 nm, where the majority of algal pigments and humic substances have their absorption peaks (Bidigare et al., 1990; Takeuchi, 2002) and where incident solar energy peaks. Algal abundance contributed some 70% to the explained variation in the bare ice reflectance data, whereas nonalgal impurities were not found to be a significant explanatory factor (supporting information Table S5). Based on the correlation results, we estimate a net reflectance reduction of 0.0380 ± 0.0035 for each algal population doubling (Figure 4; supporting information Table S4).

4. Discussion

Our analysis shows that surface ice algae have a more significant impact than nonalgal impurities on bare ice albedo across the study area of the Greenland ice sheet. The dominance of algae in the albedo signal is demonstrated by the stronger correlation between the algal fraction and albedo compared with the nonalgal fraction and by the fact that algal abundance explained $\sim 70\%$ of variation in the bare ice reflectance data, whereas nonalgal impurities were not a significant explanatory factor. The nonalgal fraction consists mostly of mineral particles and also contains black carbon and other organic material, such as small microbial cells and products of cell metabolism and decay. Hence, the absorption attributed to nonalgal impurities may still

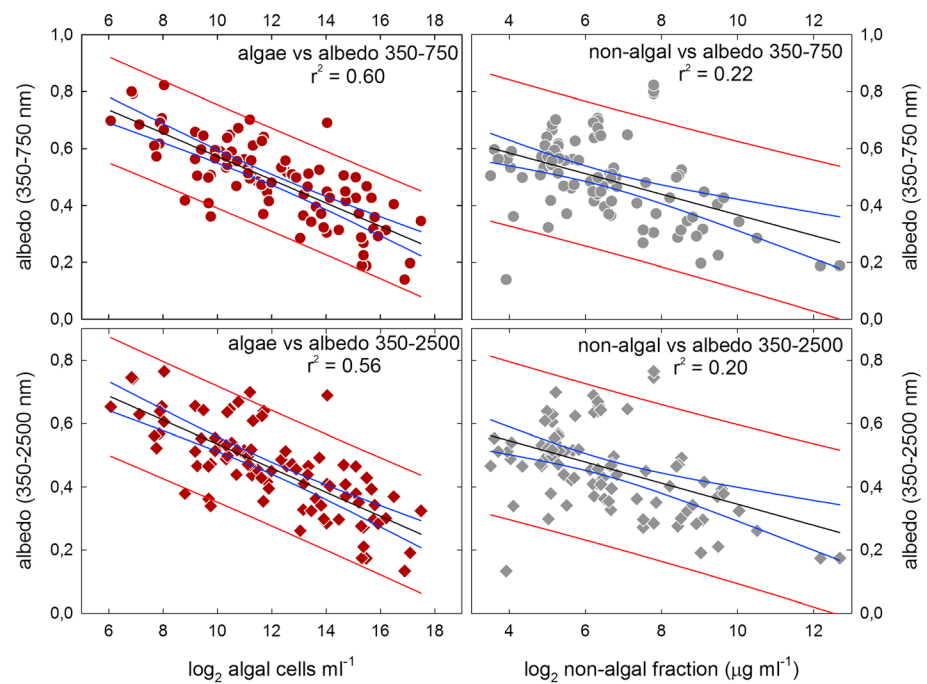


Figure 4. The effect of the algal and nonalgal fraction concentrations on bare ice albedo on the Greenland ice sheet according to our observations. The 95% confidence and prediction bands are marked in blue and red, respectively, $n = 93$.

contain a small biotic element. Direct microscopic observation from melted ice samples supports the important role of surface ice algae on bare ice albedo as they demonstrate dark algal cells contrasting with translucent mineral particles (Figures 1e–1g). These observations agree with independent spectroscopy measurements of single algal cells and mineral particles (Yallop et al., 2012).

BC is an effective LAI and has been proposed as an important factor affecting albedo (Keegan et al., 2014). In our analysis, BC is attributed to the nonalgal fraction that does not appear to significantly impact on bare ice reflectance variance (supporting information Table S5). This might be due to the way the nonalgal LAI fraction is determined in our study, as the potential effect of BC could be masked by other nonabsorbing impurities in the fraction. However, given the low BC concentrations in our samples and elsewhere on the Greenland ice sheet (Doherty et al., 2010) and the recent analysis suggesting the role of BC deposition in albedo change on the ice sheet is not significant (Tedesco et al., 2016), we propose that the effect of BC on bare ice albedo across the study area is subtle and secondary to that of algal biomass.

Cryoconite (glacier surface debris) granules, formed by microbial aggregation (Langford et al., 2010; Takeuchi et al., 2001), may contain >5% of organic carbon (Stibal et al., 2010) and have been found to decrease reflectance in laboratory experiments (Musilova et al., 2016). An association between cryoconite coverage and bare ice albedo has also been observed on the ice sheet (Chandler et al., 2015). However, cryoconite holes are hidden from nonzenith solar illumination angles and aerial imagery indicates that they only occupy a very small fractional area of the ice surface, meaning that they are of secondary importance for bare ice albedo to distributed impurities (Ryan et al., 2016).

The main factors controlling algal growth in surface ice are the presence of liquid water, light, and nutrient availability (Lutz et al., 2014; Stibal et al., 2012; Yallop et al., 2012). Dust melting out from old ice may play an important role as a source of nutrients for growing algae. Significant amounts of phosphorus, which is a limiting nutrient in supraglacial ecosystems (Stibal et al., 2009), have been detected in dust outcropping in the study area (Wientjes et al., 2011). Moreover, our redundancy analysis identified dust as contributing 9.5% to the explained variation in algal abundance and biovolume data (supporting information Table S2). Significant correlation was also found between dust content and the abundance of microbes in ice sheet surface ice (Stibal et al., 2015). Hence, algal growth rates on the ice sheet are likely to be dependent on surface dust concentration, and consequently, algal hot spots may be concentrated in areas with high dust

concentrations. However, surface ice algae are also found outside the dark area and so these areas should not be excluded when estimating the algal contribution to the ice sheet surface darkening.

5. Conclusions

We conclude that actively growing pigmented algae have a significant impact on albedo reduction in the study area in the southwestern part of the Greenland ice sheet and that this impact is more important than that of other light-absorbing impurities such as dust or black carbon. Upscaling ice darkening due to algal growth over the entire ice sheet and incorporating this effect into radiative forcing models is expected to improve mass balance, runoff, and sea level projections from Greenland and other ice masses elsewhere.

Acknowledgments

This research is part of the Dark Snow Project (<http://darksnow.org>). It was funded by Villum Young Investigator Programme grant VKR 023121 to M. S., the Leonardo DiCaprio Foundation, and more than 700 crowd funders, and M. S. was additionally supported by Marie Skłodowska-Curie Individual Fellowship 657533 (EMoGrIS). We acknowledge crowd funding and media support from Peter Sinclair and field assistance from Gabriel Warren and Martyn Law. The Programme for Monitoring of the Greenland Ice Sheet (www.PROMICE.dk), Greenland Analogue Project (GAP), and the K-transect AWS program of UU/IMAU made in situ automated climate station observations available. Ellen Mosley-Thompson and Michelle Cook (Ohio State University) and Waleed Abdalati (University of Colorado) provided ASD spectrometers used in the study. We also thank Anne Nolin (Oregon State University) for tips for interpreting absorption features, Joshua Schwarz (National Oceanic and Atmospheric Administration) for black carbon analysis support, and Marie Dumont (National Centre for Meteorological Research) for spectral weighting tips. The data used in this study are available as a supporting information data set.

References

- Ahlström, A. P., Gravesen, P., Andersen, S. B., van As, D., Citterio, M., Fausto, R. S., ... Petersen, D. (2008). A new programme for monitoring the mass loss of the Greenland ice sheet. *Geological Survey of Denmark and Greenland Bulletin*, 15, 61–64.
- Baumgardner, D., Popovicheva, O., Allan, J., Bernardoni, V., Cao, J., Cavalli, F., ... Viana, M. (2012). Soot reference materials for instrument calibrations and comparisons. *Atmospheric Measurement Techniques*, 5(2), 2315–2362. <https://doi.org/10.5194/amt-5-1869-2012>
- Benning, L. G., Anesio, A. M., Lutz, S., & Tranter, M. (2014). Biological impact on Greenland's albedo. *Nature Geoscience*, 7(10), 691. <https://doi.org/10.1038/ngeo2260>
- Bidigare, R. R., Ondrusek, M. E., Morrow, J. H., & Kiefer, D. A. (1990). In vivo absorption properties of algal pigments. *SPIE Ocean Optics*, 1302, 290–302. <https://doi.org/10.1117/12.21451>
- Bøggild, C. E., Brandt, R. E., Brown, K. J., & Warren, S. G. (2010). The ablation zone in northeast Greenland: Ice types, albedos and impurities. *Journal of Glaciology*, 56(195), 101–113. <https://doi.org/10.3189/002214310791190776>
- Bond, T. C., & Bergstrom, R. W. (2006). Light absorption by carbonaceous particles: An investigative review. *Aerosol Science and Technology*, 40(1), 27–67. <https://doi.org/10.1080/02786820500421521>
- Box, J. E. (1997). Polar day effective cloud opacity in the Arctic derived from measured and modeled solar radiation fluxes, MA thesis, Department of Geography, University of Colorado, Boulder, cooperative Institute for Research in Environmental Sciences (111 pp.).
- Box, J. E., Fettweis, X., Stroeve, J. C., Tedesco, M., Hall, D. K., & Steffen, K. (2012). Greenland ice sheet albedo feedback: Thermodynamics and atmospheric drivers. *The Cryosphere*, 6(4), 821–839. <https://doi.org/10.5194/tc-6-821-2012>
- Bryant, D. A. (1982). Phycoerythrocyanin and phycoerythrin: Properties and occurrence in cyanobacteria. *Journal of General Microbiology*, 128(4), 835–844. <https://doi.org/10.1099/00221287-128-4-835>
- Chandler, D. M., Alcock, J. D., Wadhams, J. L., Mackie, S. L., & Telling, J. (2015). Seasonal changes of ice surface characteristics and productivity in the ablation zone of the Greenland ice sheet. *The Cryosphere*, 9(2), 487–504. <https://doi.org/10.5194/tc-9-487-2015>
- Doherty, S. J., Grenfell, T. C., Forsström, S., Hegg, D. L., Brandt, R. E., & Warren, S. G. (2013). Observed vertical redistribution of black carbon and other insoluble light-absorbing particles in melting snow. *Journal of Geophysical Research: Atmospheres*, 118, 5553–5569. <https://doi.org/10.1002/jgrd.50235>
- Doherty, S. J., Warren, S. G., Grenfell, T. C., Clarke, A. D., & Brandt, R. E. (2010). Light-absorbing impurities in Arctic snow. *Atmospheric Chemistry and Physics*, 10(23), 11,647–11,680. <https://doi.org/10.5194/acp-10-11647-2010>
- Fettweis, X., Tedesco, M., van den Broeke, M., & Ettema, J. (2011). Melting trends over the Greenland ice sheet (1958–2009) from spaceborne microwave data and regional climate models. *The Cryosphere*, 5(2), 359–375. <https://doi.org/10.5194/tc-5-359-2011>
- Goelles, T., Bøggild, C. E., & Greve, R. (2015). Ice sheet mass loss caused by dust and black carbon accumulation. *The Cryosphere*, 9(5), 1845–1856. <https://doi.org/10.5194/tc-9-1845-2015>
- Hadley, O. L., & Kirchstetter, T. W. (2012). Black-carbon reduction of snow albedo. *Nature Climate Change*, 2(6), 437–440. <https://doi.org/10.1038/nclimate1433>
- Hillebrand, H., Dürselen, C.-D., Kirschtel, D., Pollinger, U., & Zohary, T. (1999). Biovolume calculation for pelagic and benthic microalgae. *Journal of Phycology*, 35(2), 403–424. <https://doi.org/10.1046/j.1529-8817.1999.3520403.x>
- Keegan, K. M., Albert, M. R., McConnell, J. R., & Baker, I. (2014). Climate change and forest fires synergistically drive widespread melt events of the Greenland ice sheet. *Proceedings of the National Academy of Sciences of the United States of America*, 111(22), 7964–7967. <https://doi.org/10.1073/pnas.1405397111>
- Langen, P. L., Mottram, R. H., Christensen, J. H., Boberg, F., Rodehacke, C. B., Stendel, M., ... Cappelen, J. (2015). Quantifying energy and mass fluxes controlling Godthåbsfjord freshwater input in a 5 km simulation (1991–2012). *Journal of Climate*, 28(9), 3694–3713. <https://doi.org/10.1175/jcli-d-14-00271.1>
- Langford, H., Hodson, A., Banwart, S., & Bøggild, C. (2010). The microstructure and biogeochemistry of Arctic cryoconite granules. *Annals of Glaciology*, 51(56), 87–94. <https://doi.org/10.3189/172756411795932083>
- Lutz, S., Anesio, A. M., Jorge Villar, S. E., & Benning, L. G. (2014). Variations of algal communities cause darkening of a Greenland glacier. *FEMS Microbiology Ecology*, 89(2), 402–414. <https://doi.org/10.1111/1574-6941.12351>
- Musilova, M., Tranter, M., Bamber, J. L., Takeuchi, N., & Anesio, A. M. (2016). Experimental evidence that microbial activity lowers the albedo of glaciers. *Geochemical Perspectives Letters*, 2, 106–116. <https://doi.org/10.7185/106%20geochemlet.1611>
- Painter, T. H., Duval, B., Thomas, W. H., Mendez, M., Heintzelman, S., & Dozier, J. (2001). Detection and quantification of snow algae with an airborne imaging spectrometer. *Applied and Environmental Microbiology*, 67(11), 5267–5272. <https://doi.org/10.1128/aem.67.11.5267-5272.2001>
- Remias, D., Holzinger, A., Aigner, S., & Lütz, C. (2012). Ecophysiology and ultrastructure of *Ancyronema nordenskiöldii* (Zygnematales, Streptophyta), causing brown ice on glaciers in Svalbard (high Arctic). *Polar Biology*, 35(6), 899–908. <https://doi.org/10.1007/s00300-011-1135-6>
- Remias, D., Schwaiger, S., Aigner, S., Leya, T., Stuppner, H., & Lütz, C. (2012). Characterization of an UV- and VIS-absorbing, purpurogallin-derived secondary pigment new to algae and highly abundant in *Mesotaenium berggrenii* (Zygnematophyceae, Chlorophyta), an extremophyte living on glaciers. *FEMS Microbiology Ecology*, 79(3), 638–648. <https://doi.org/10.1111/j.1574-6941.2011.01245.x>
- Ricchiazzi, P., Yang, S., Gautier, C., & Sowle, D. (1998). SBDART: A research and teaching software tool for plane-parallel radiative transfer in the Earth's atmosphere. *Bulletin of the American Meteorological Society*, 79(10), 2101–2114. [https://doi.org/10.1175/1520-0477\(1998\)079](https://doi.org/10.1175/1520-0477(1998)079)

- Ryan, J. C., Hubbard, A. L., Box, J. E., Todd, J., Christoffersen, P., Carr, J. R., ... Snooke, N. (2015). UAV photogrammetry and structure from motion to assess calving dynamics at store glacier, a large outlet draining the Greenland ice sheet. *The Cryosphere*, 9(1), 1–11. <https://doi.org/10.5194/tc-9-1-2015>
- Ryan, J. C., Hubbard, A., Stibal, M., & Box, J. E. (2016). Attribution of Greenland's ablating ice surfaces on ice sheet albedo using unmanned aerial systems. *The Cryosphere Discussions*, 1–23. <https://doi.org/10.5194/tc-2016-204>
- Schwarz, J. P., Doherty, S. J., Li, F., Ruggiero, S. T., Tanner, C. E., Perring, A. E., ... Fahey, D. W. (2012). Assessing recent measurement techniques for quantifying black carbon concentration in snow. *Atmospheric Measurement Techniques*, 5(11), 2581–2592. <https://doi.org/10.5194/amt-5-2581-2012>
- Shimada, R., Takeuchi, N., & Aoki, T. (2016). Inter-annual and geographical variations in the extent of bare ice and dark ice on the Greenland ice sheet derived from MODIS satellite images. *Frontiers in Earth Science*, 4, 43. <https://doi.org/10.3389/feart.2016.00043>
- Stibal, M., Anesio, A. M., Blues, C. J. D., & Tranter, M. (2009). Phosphatase activity and organic phosphorus turnover on a high Arctic glacier. *Biogeosciences*, 6(5), 913–922. <https://doi.org/10.5194/bg-6-913-2009>
- Stibal, M., Gözdereliler, E., Cameron, K. A., Box, J. E., Stevens, I. T., Gokul, J. K., ... Jacobsen, C. S. (2015). Microbial abundance in surface ice on the Greenland ice sheet. *Frontiers in Microbiology*, 6, 225. <https://doi.org/10.3389/fmicb.2015.00225>
- Stibal, M., Lawson, E. C., Lis, G. P., Mak, K. M., Wadham, J. L., & Anesio, A. M. (2010). Organic matter content and quality in supraglacial debris across the ablation zone of the Greenland ice sheet. *Annals of Glaciology*, 51(56), 1–8. <https://doi.org/10.3189/172756411795931958>
- Stibal, M., Šabacká, M., & Žárský, J. (2012). Biological processes on glacier and ice sheet surfaces. *Nature Geoscience*, 5(11), 771–774. <https://doi.org/10.1038/ngeo1611>
- Takeuchi, N. (2002). Optical characteristics of cryoconite (surface dust) on glaciers: The relationship between light absorbency and the property of organic matter contained in the cryoconite. *Annals of Glaciology*, 34, 409–414. <https://doi.org/10.3189/172756402781817743>
- Takeuchi, N., Fujisawa, Y., Kadota, T., Tanaka, S., Miyairi, M., Shirakawa, T., ... Ohata, T. (2015). The effect of impurities on the surface melt of a glacier in the Suntar-Khayata mountain range, Russian Siberia. *Frontiers in Earth Science*, 3, 82. <https://doi.org/10.3389/feart.2015.00082>
- Takeuchi, N., Kohshima, S., & Seko, K. (2001). Structure, formation, and darkening process of albedo-reducing material (cryoconite) on a Himalayan glacier: A granular algal mat growing on the glacier. *Arctic, Antarctic, and Alpine Research*, 33(2), 115–122. <https://doi.org/10.2307/1552211>
- Tedesco, M., Doherty, S., Fettweis, X., Alexander, P., Jeyaratnam, J., & Stroeve, J. (2016). The darkening of the Greenland ice sheet: Trends, drivers, and projections (1981–2100). *The Cryosphere*, 10(2), 477–496. <https://doi.org/10.5194/tc-10-477-2016>
- van den Broeke, M. R., Smeets, C. J. P. P., & van de Wal, R. S. W. (2011). The seasonal cycle and interannual variability of surface energy balance and melt in the ablation zone of the west Greenland ice sheet. *The Cryosphere*, 5, 377–390. <https://doi.org/10.5194/tc-5-377-2011>
- van As, D., Fausto, R. S., Cappelen, J., van de Wal, R. S. W., Braithwaite, R. J., Machguth, H., & the PROMICE project team (2016). Placing Greenland ice sheet ablation measurements in a multi-decadal context. *Geological Survey of Denmark and Greenland Bulletin*, 35, 71–74.
- Wientjes, I. G. M., & Oerlemans, J. (2010). An explanation for the dark region in the western melt zone of the Greenland ice sheet. *The Cryosphere*, 4(3), 261–268. <https://doi.org/10.5194/tc-4-261-2010>
- Wientjes, I. G. M., van de Wal, R. S. W., Reichert, G. J., Sluijs, A., & Oerlemans, J. (2011). Dust from the dark region in the western ablation zone of the Greenland ice sheet. *The Cryosphere*, 5(3), 589–601. <https://doi.org/10.5194/tc-5-589-2011>
- Yallop, M. L., Anesio, A. M., Perkins, R. G., Cook, J., Telling, J., Fagan, D., ... Roberts, N. W. (2012). Photophysiology and albedo-changing potential of the ice algal community on the surface of the Greenland ice sheet. *The ISME Journal*, 6(12), 2302–2313. <https://doi.org/10.1038/ismej.2012.107>